

Origin of the Drastic Current Decay during Potentiostatic Alkaline Methanol Oxidation

Theresa Haisch, Fabian Kubannek, Dejun Chen, YuYe J. Tong, and Ulrike Krewer*

ABSTRACT: The current production from the alkaline methanol electro oxidation reaction does not reach a steady state on a smooth platinum catalyst under potentiostatic conditions. We investigated two possible explanations for this phenomenon: changes on the catalyst surface and changes in the solution near the electrode. In situ Fourier transform infrared spectroscopy experiments were conducted to evaluate the adsorbed species on the catalyst surface and a simulation model was set up to describe the changes of concentrations inside the solution. Linear and bridge bonded carbon monoxide are the only organic compounds which can be detected by in situ spectroscopy at fixed potentials, but their amount does not increase over time. The simulation shows that the consumption of hydroxide ions and production of carbonaceous species during alkaline oxidation causes a local pH shift near the catalyst surface. Assuming a one electron transfer as the limiting step, this pH shift was found to contribute to the observed current loss at a potential of 0.77 V.

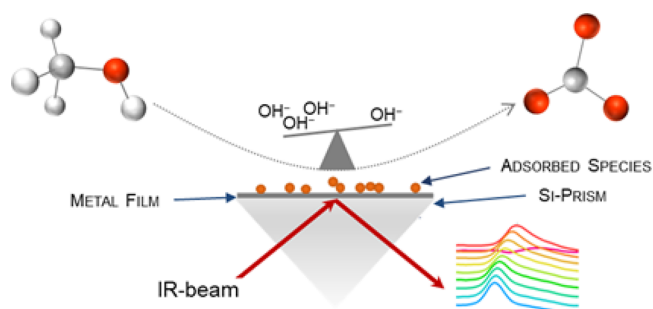
KEYWORDS: local pH shift, alkaline electrolyte, methanol electrooxidation, ATR SEIRAS, FTIR spectroscopy

INTRODUCTION

Methanol is an attractive candidate as a fuel for the use in fuel cells because of its high volumetric energy density (15.9 MJ L^{-1}) and reduced safety risks compared to hydrogen.^{1,2} Most systems with alcohol as a fuel use acidic electrolytes. However, the methanol oxidation reaction (MOR) in alkaline media benefits from improved kinetics.^{3,4} Also, the reaction kinetics of the oxygen reduction, which takes place at the cathode of a direct methanol fuel cell, is enhanced in alkaline solutions.⁵

Investigations of the alkaline MOR on platinum electrodes have shown that no stationary state is achievable under potentiostatic conditions because the current does not become constant.^{6,7} A continuous current drop is observed which can, in principle, be caused by two factors: a change of the catalyst surface or a change in the solution near the catalyst. Changes of the catalyst surface could result from (a) a restructuring or oxidation of the platinum atoms, (b) the deposition of metal impurities, and (c) chemisorption of blocking reaction intermediates. Changes in the solution composition near the surface could result from (d) anion physisorption of carbonate ions formed from the MOR reaction product CO_2 or (e) the consumption of reaction educts, methanol, and hydroxide ions.

Each of these processes can have a strong influence on the electrode reaction in a particular potential, pH, or temperature range, or in a particular electrolyte. In this work, we focus on factors that cause a current decline during the alkaline MOR under typical electrochemical measurement conditions, that is,



on a platinum catalyst in an electrolyte containing only NaOH and methanol. We further limit the analysis to a temperature of $25 \text{ }^\circ\text{C}$ and a pH value of 13, which are both common reaction conditions. Under these conditions, option (a) can be excluded because the decline in current density occurs for platinum bulk metal without any support, and even at potentials below the range of platinum oxide formation, as the Pourbaix diagram indicates (see Figure S1 in Supporting Information).^{8,9} In addition, we did not find indications for a further restructuring mechanism of platinum in the MOR potential range. The deposition of metal impurities can be avoided by using high purity chemicals. Also the use of non glass equipment reduces the presence of contaminants.^{6,10,11} Furthermore, the current density also declines at potentials above 0.8 V versus reversible hydrogen electrode (RHE) where impurities would dissolve rather than precipitate. Thus explanation (b) is most unlikely.

Explanation (d) can be rejected based on the fact that the MOR in a sodium carbonate electrolyte reaches the same current density as in a sodium hydroxide electrolyte (see Figure S2a in Supporting Information). CA curves in a

on a platinum catalyst in an electrolyte containing only NaOH and methanol. We further limit the analysis to a temperature of $25 \text{ }^\circ\text{C}$ and a pH value of 13, which are both common reaction conditions. Under these conditions, option (a) can be excluded because the decline in current density occurs for platinum bulk metal without any support, and even at potentials below the range of platinum oxide formation, as the Pourbaix diagram indicates (see Figure S1 in Supporting Information).^{8,9} In addition, we did not find indications for a further restructuring mechanism of platinum in the MOR potential range. The deposition of metal impurities can be avoided by using high purity chemicals. Also the use of non glass equipment reduces the presence of contaminants.^{6,10,11} Furthermore, the current density also declines at potentials above 0.8 V versus reversible hydrogen electrode (RHE) where impurities would dissolve rather than precipitate. Thus explanation (b) is most unlikely.

carbonate containing solution shows similar decline behavior as in a NaOH based solution (see Figure S2b in [Supporting Information](#)). Therefore, carbonates do not lead to toxication of the system and cannot be the reason of the current decrease.⁶ The remaining two explanations, (c,e) are both supported by the literature and will be tested in detail in this work.

Matsuoka et al. suggested that the continuous current decrease during alkaline MOR is caused by adsorbed CO.⁷ The reaction intermediate reduces the active area by blocking free sites of the platinum catalyst like it is known from the MOR in acid media.¹² Another option explaining the continuous current decrease is an alteration of the electrolyte composition because of the consumption of hydroxide ions and production of carbonaceous species which might cause a local pH shift near the electrode surface. Lai et al. and Figueiredo et al. reported a pH shift by up to 1.3 units near the catalyst/electrolyte interphase for ethanol oxidation in an alkaline electrolyte.^{13,14} The pH shift could change the reaction kinetics as well as the reaction mechanism and product distribution.

The first hypothesis which we analyze in this work is the surface blocking effect of adsorbed intermediates. Fourier transform infrared (FTIR) spectroscopy is a common technique to identify adsorbed intermediates and can be combined with electrochemical methods. Morallón et al. studied the alkaline methanol oxidation under potentiodynamic conditions in combination with FTIR spectroscopy and found formate (1385 and 1580 cm^{-1}), bicarbonate (1360 cm^{-1}), carbon dioxide (2343 cm^{-1}), and linear as well as bridge bonded carbon monoxide (2000 and 1800 cm^{-1}).¹⁵ Their results were confirmed by Zhou et al. who, additionally, determined carbonate (1380 cm^{-1}) and a second band resulting from bicarbonate (1673 cm^{-1}).¹⁶ In a previous study, we also found formate, carbonate, and bicarbonate as species near the electrode surface during a CV scan.⁶ In contrast to the reported FTIR results where species within a thin solvent layer near the catalyst surface were detected, we used in situ attenuated total reflection surface enhanced IR reflection absorption spectroscopy (ATR SEIRAS) which enables the detection of adsorbed species solely. Because of required laborious preparation and the poor stability of the ultrathin platinum film used as the working electrode, this technique is rarely used for investigations in alkaline electrolytes. In our study, we investigate potentiostatic conditions because it is not yet known in detail how the coverage of surface species is developing with time at a fixed potential. Therefore, chronoamperometric measurements combined with in situ FTIR spectroscopy were performed.

The second hypothesis postulates that a change in the solution composition causes the current density decline. The effect of impurities can be neglected because they contribute to the loss only at the beginning of the measurement but not as a continuous factor.⁶ Near the electrode surface, methanol depletion or a local pH change because of the consumption of hydroxide ions and production of (bi)carbonates can occur. The change of the pH influences the local environment of the reaction and thereby directly affects the reaction pathway and resulting species.^{17,18} A higher pH accelerates the reaction kinetics so that a reduction of the pH is followed by a slower kinetic and reduced reaction rate of the electrochemical reaction. Simulations of Schröder and Krewer showed for alkaline zinc air cells that the carbonation of the alkaline electrolyte rapidly consumes hydroxides, and thus prevents any

long term stable operation.¹⁹ Furthermore, a decrease in pH might significantly increase the equilibrium potential. This was demonstrated by a physical model for the alkaline membrane fuel cell operated with air containing CO₂.¹⁸ Carbonate accumulated in the electrolyte shifted the potential up to 180 mV. Based on this relation, we expect that a pH shift can be a source for the constant current decline.

In order to evaluate the theoretically expectable influence of a pH shift or methanol depletion on the recorded current, we set up a physical model. This allows to avoid a direct measurement of local conditions which would be difficult to realize. The model provides a basis for a first study to explain the continuous current decay and is not contemplated for a complete kinetic model study. The results of the simulation are intended to give information about the behavior of the current–time curve, in particular of the influence of concentration shifts after longer running times.

■ MATERIALS AND METHODS

Chemicals. All chemicals used in this work, NaOH (Sigma Aldrich, 99.99% trace metal basis), methanol (VWR, HPLC grade or Fisher Chemicals, 99.8% ACS Reagent Grade), ammonium fluoride (Alfa Aesar, 96%), platinum(II) chloride (Pressure Chemicals Co., 73% Pt), ammonium hydroxide (Fisher Chemicals, ACS Plus Grade), hydrofluoric acid (Alfa Aesar, ACS), and the deuterated species CD₃OD, NaOD, and D₂O (Cambridge Isotope LABS, 99–99.9%), were used without any further purification. All solutions were freshly prepared on a daily basis with Milli Q water (18.2 MΩ).

Fabrication of the Platinum Catalyst Film. The working electrode consists of an ultrathin (ca. 90 nm) platinum film deposited on a silicon prism by electroless plating.^{20,21} The Si prism (20 mm × 25 mm) works as an optical window for the ATR SEIRAS and has to be cleaned thoroughly prior to the film formation. For that, it is polished with finer grade alumina slurries down to 0.3 μm, starting with 5 μm, and sonicated in Milli Q water to remove all excess particles. Afterward, the Si prism was immersed into a 5% NH₄F solution for about 1 min to etch the surface creating a hydrophobic top. Platinum (II) (95 mg) chloride was dissolved in 8.66 mL of Milli Q water with 1.34 mL of ammonium hydroxide for the Pt precursor solution. Pt(II)–chloride is almost insoluble in water, which is why ammonium hydroxide is added to dissolve the solid. The resulting suspension was heated at 60 °C for about 2 h. In between, it was placed into an ultrasonic bath to ensure a complete dissolution. The Pt precursor solution (513 μL) was added to a mixture of 450 μL hydrofluoric acid and 3.537 mL Milli Q water. Subsequently, 3 mL of the mixture was deposited onto the Si prism surface which had been preheated to 60 °C in advance. With the hydrofluoric acid SiF₆²⁻ is formed from Si in order to reduce Pt(II) to the Pt film.²⁰ The film formation took about 15 min. Afterward, the newly formed Pt surface was washed with Milli Q water to remove waste solution, and subsequently air dried by N₂ gas. The platinum film has high sensitivity to alkaline media, and therefore the maximum pH value of the electrolyte is limited to 13 in order to obtain sufficient stability during FTIR measurements.

Electrochemical and Spectroscopic Measurements. The electrochemical experiments combined with FTIR spectroscopy were performed in a homemade three electrode cell using a Pt gauze as the counter and a Ag/AgCl (3 M, BASi) as the reference electrode connected with a CHI 601D potentiostat. For the recording of in situ FTIR spectra, an Agilent 670 IR spectrometer with a spectral resolution of 4 cm^{-1} was used. A spectrometer was equipped with a liquid nitrogen cooled mercury–cadmium–telluride detector. All IR spectra are defined in absorbance units as $-\log(I/I_0)$. The electrochemical measurements using a rotating disc electrode were performed with a three electrode cell setup (PINE Instruments) with platinum working and counter electrodes. If possible the set up components do not consist of glass to avoid impurities from glass.⁶ A RHE served as the reference electrode (Gaskatel). The currents were

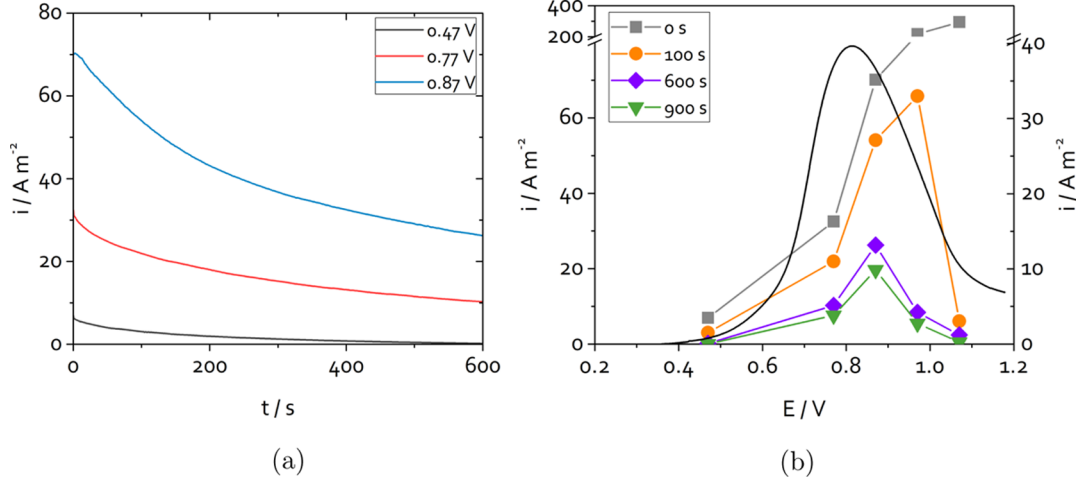


Figure 1. (a) Current–time curve of a 0.1 M NaOH + 0.1 M MeOH solution at different potentials (0.47, 0.77, and 0.87 V) on a smooth platinum RDE at 100 rpm. (b) Current densities during CA measurements (left axis) at selected points in time in a potential range of 0.47–1.07 V and linear sweep curve (right axis) with a scan rate of 10 mV s⁻¹.

recorded with a Zennium X potentiostat (Zahner Elektrik GmbH). All presented potentials are referred to the RHE. Prior to all electrochemical measurements, the solution was purged with nitrogen and the working electrode was cleaned electrochemically as described elsewhere.⁶ If not stated otherwise, the measurements were conducted at 25 °C with a concentration of 0.1 M NaOH and 0.1 M MeOH.

Modeling. In this section, we present the physical and mathematical backgrounds for our model describing the influence of the electrolyte changes on the current during alkaline MOR. The complete alkaline methanol oxidation $\text{CH}_3\text{OH} + 6\text{OH}^- \rightarrow \text{CO}_2 + 5\text{H}_2\text{O} + 6\text{e}^-$ leads to the formation of carbon dioxide. Under strongly alkaline conditions, carbon dioxide rapidly transforms into carbonate $\text{CO}_2 + 2\text{OH}^- \rightarrow \text{CO}_3^{2-} + \text{H}_2\text{O}$. Both reactions involve CO_2 and the consumption of hydroxide ions and thus cause a local change in the electrolyte composition. According to the literature, the rate limiting step of the alkaline MOR can be chemical or electrochemical depending on the applied potential. Considering that only the potential ranges limited by electron transfer result in a Tafel slope of 120 mV dec⁻¹.^{22,23} This is a typical value of a one electron transfer as the rate determining step.

The influence of the electrolyte change on the current density is described by a physical chemical model. The applied potential is large and thus conditions are far away from open circuit potential. The backward reaction is neglected and a lumped Tafel type methanol oxidation kinetic is assumed

$$i = i_0 \cdot \left(\frac{c_{\text{OH}}}{c_{\text{bulk,OH}}} \right) \cdot \left(\frac{c_{\text{MeOH}}}{c_{\text{bulk,MeOH}}} \right) \cdot \exp \left(\frac{\alpha \cdot (E - E^0) \cdot F}{RT} \right) \quad (1)$$

i and i_0 represent the current density (A cm⁻²) and the exchange current density (A cm⁻²), respectively. The other parameters characterize the hydroxide surface concentration c_{OH} /hydroxide bulk concentration $c_{\text{bulk,OH}}$ and methanol surface concentration c_{MeOH} /methanol bulk concentration $c_{\text{bulk,MeOH}}$ (all mol L⁻¹), charge transfer coefficient α (≈ 0.5), applied electrode potential E (V), open circuit potential E^0 (V), Faraday constant F (C mol⁻¹), universal gas constant R (J K⁻¹ mol⁻¹), and temperature T (K). The open circuit potential E^0 is calculated by the Nernst equation (eq 2)

$$E^0 = E^{00} + \frac{RT}{6F} \ln \frac{a_{\text{CO}_2} \cdot a_{\text{H}_2\text{O}}^5}{a_{\text{CH}_3\text{OH}} \cdot a_{\text{OH}^-}^6} \quad (2)$$

Dilute solution behavior is assumed, which allows to set the water activity $a_{\text{H}_2\text{O}}$ equal to one and replace the remaining activities with concentrations normalized with a reference concentration c_0 of 1 mol L⁻¹. In another work we found that activities instead of

concentrations and Maxwell–Stefan diffusion instead of Fick’s law of diffusion need to be used in highly concentrated NaOH electrolyte.²⁴ At the experimental concentration of 0.1 M, the theory of the dilute solution can be applied. The hydroxide ion concentration c_{OH} can be replaced by the proton concentration using the relation $c_{\text{OH}} \cdot c_{\text{H}^+} = 10^{-14}$ mol² L⁻². The influence of methanol is much lower than that of OH⁻ because it appears with an exponent of six in the equation and, thus, is neglected. Finally, our experiments with deuterated species, which are discussed in the result section, show that OH⁻ has a larger influence than methanol under the investigated conditions. The conversion of the hydroxide concentration into the corresponding proton concentration enables to transform the Nernst equation into a form which includes the pH value.

$$E_{0,t} - E_{0,t=0} \approx \frac{RT}{6F} \ln \frac{1}{a_{\text{OH}^-,t}^6} - \frac{RT}{6F} \ln \frac{1}{a_{\text{OH}^-,t=0}^6} = 59 \text{ mV} \cdot \Delta\text{pH}$$

$$\text{with } \Delta\text{pH} = \text{pH}_t - \text{pH}_{t=0} \quad (3)$$

$$E^0 \approx E_2^{00} + 59 \text{ mV} \cdot \Delta\text{pH} \quad (4)$$

E_2^{00} involves the conversion of the hydroxide concentration to the corresponding proton concentration as well as the conversion into pH. Inserting E^0 into the Tafel equation and rearranging the equation yields

$$i = i_0 \cdot \left(\frac{c_{\text{OH}}}{c_{\text{bulk,OH}}} \right) \cdot \left(\frac{c_{\text{MeOH}}}{c_{\text{bulk,MeOH}}} \right) \cdot \exp \left(\frac{\alpha \cdot (E - E_2^{00} - 59 \text{ mV} \cdot \Delta\text{pH}) \cdot F}{RT} \right) \quad (5)$$

For constant potential operation, the constant terms E and E_2^{00} can be included in the pre exponential factor yielding the final kinetic expression

$$i = i_0^* \cdot \left(\frac{c_{\text{OH}}}{c_{\text{bulk,OH}}} \right) \cdot \left(\frac{c_{\text{MeOH}}}{c_{\text{bulk,MeOH}}} \right) \cdot \exp \left(\frac{-\alpha \cdot 59 \text{ mV} \cdot \Delta\text{pH} \cdot F}{RT} \right) \quad (6)$$

The diffusive transport of hydroxide ions and methanol perpendicular to the electrode surface is considered in the model by

$$\frac{dc_{\text{OH}}}{dt} = -D_{\text{OH}} \frac{\partial^2 c_{\text{OH}}}{\partial x^2} \quad (7)$$

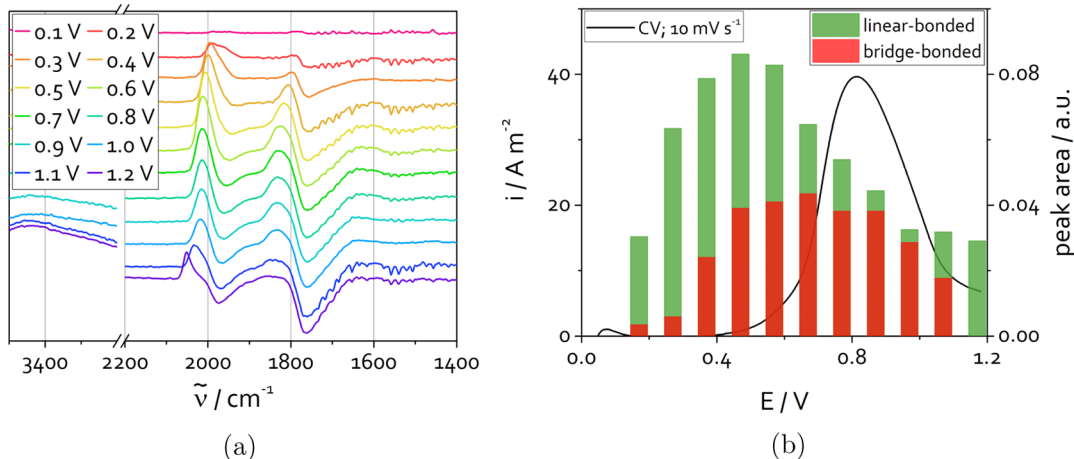


Figure 2. (a) In situ FTIR spectra of a 0.1 M NaOH + 0.1 M MeOH solution on a thin platinum film catalyst during potentiodynamic measurement between 0.1 and 1.2 V vs RHE (forward scan). (b) Corresponding CV curve (solid line) and the integrated IR band intensities of adsorbed bridge and linear bonded CO.

$$\frac{dc_{\text{MeOH}}}{dt} = -D_{\text{MeOH}} \frac{\partial^2 c_{\text{MeOH}}}{\partial x^2} \quad (8)$$

D is the diffusion coefficient of hydroxide ions ($5 \times 10^{-9} \text{ m}^2 \text{ s}^{-1}$) and methanol ($1.3 \times 10^{-9} \text{ m}^2 \text{ s}^{-1}$), respectively, in the solution at an experimental temperature of 25 °C.²⁵ The boundary layer thickness δ_N is calculated with²⁶

$$\delta_N = 1.61\omega^{-1/2}\nu^{1/6}D_{\text{OH}}^{1/3} \quad (9)$$

which derives from the Levich equation, where ω is the rotation rate of the electrode (100 rpm) and ν is the kinematic viscosity of the electrolyte which is set equal to the viscosity of water ($0.893 \times 10^{-6} \text{ m}^2 \text{ s}^{-1}$) at 25 °C because of the low electrolyte concentration.²⁷ The following boundary conditions are used to solve the transport problem

$$c_{\text{OH}}|_{x=\delta_N} = c_{\text{OH},0} \quad (10)$$

$$-D_{\text{OH}} \frac{\partial c_{\text{OH}}}{\partial x} \Big|_{x=0} = \frac{8}{6} i \quad (11)$$

For pH values above 11.5, nearly 100% of the CO_2 will be present as carbonate. Therefore, the factor 8/6 is added because eight hydroxide ions are consumed by the electrochemical reaction for every methanol molecule. The six in the denominator represents the number of total electrons transferred per methanol molecule.

The model is implemented and solved in the software Matlab. The partial differential equation is discretized using a finite volume scheme with 1000 mesh elements. We simulated the case with the limiting step as a one electron transfer. For the starting conditions, the concentration at the surface is the same as in the bulk because no reaction is assumed to take place before and the pH value is constant, the current density i becomes equal to i_0^* . Thus, i_0^* is set to the initial value of the experimental current.

RESULTS AND DISCUSSION

Electrochemical measurements of alkaline MOR under potentiostatic conditions reveal a continuous current density loss with time over a wide potential window. Figure 1a shows the current density at 0.77 V over time of a 0.1 M alkaline methanol solution in the rotating disk electrode (RDE) cell. This potential corresponds to the relevant potential window of methanol oxidation.⁶ In Figure 1b, the linear sweep curve of the alkaline MOR shows that at potentials below 0.4 V, there is no MeOH oxidation yet. This is assigned to blocking intermediates.²⁸ Between 0.4 and 0.8 V, the MOR takes

place. Above that the current declines again. The decline is assigned to the formation of Pt oxides that deactivate the catalyst.⁸ It can be observed that the current density decreases over the entire measuring time with the slope depending on time and applied potential. Also, the application of other potentials results in a similar observation. None of the recorded CA curves reaches a steady state behavior within 10 min (Figure 1b).

Hypothesis One: Blocking Intermediates. To test the hypothesis of catalyst deactivation by blocking intermediates, in situ FTIR spectra were recorded under potentiodynamic and potentiostatic conditions. FTIR spectroscopy provides information about adsorbed species on the catalyst and might indicate catalyst blocking intermediates. It is assumed that reaction intermediates of the alkaline MOR are adsorbed on the catalyst surface but the desorption is hindered so that the organic species work as a catalyst poison. The existence of different intermediates has been confirmed before.^{6,15,16} Our intention is to evaluate how far they act as a catalyst poison. The recording of CV curves gives an overview of the potential dependent occurrence of intermediates and products, whereas CA curves provide information about the temporal change of the surface coverage.

Figure 2a illustrates IR spectra that were taken every 0.1 V while a cyclic voltammetry forward scan was running. A total of four bands are detected. The broadband around 3500 cm^{-1} characterizes OH vibrations. The band at 1630 cm^{-1} is located in an area typical for carbonyl vibrations but also for deformation vibrations of OH bonds. The comparison with FTIR spectra resulting from an isotope labeled methanol solution ($\text{C}^{13}\text{H}_3\text{OH}$) shows no changes of this band position and therefore proves that the band can be assigned to OH oscillation (Figure S3 in the Supporting Information). The position of the other two bands, 1810 and 2000 cm^{-1} is affected by the use of $\text{C}^{13}\text{H}_3\text{OH}$ and, therefore, they can be connected to carbon containing bonds, in detail they belong to linear and bridge bonded carbon monoxide.¹⁵ Table 1 shows the assignment of the bands to the vibrations. The position of both carbonyl IR bands depends on the potential. These shifts, which are in the range around $50\text{--}60 \text{ cm}^{-1}$ in the forward scan, are based on a combination of two effects: the Stark effect and a coverage dependent shift (more information can be found in the Supporting Information).^{29–31} CO is the only

Table 1. FTIR Peak Values of Methanol Electrooxidation

wave number/cm ⁻¹	type of vibration
3000 3500	ν (OH)
2000/1940	ν (CO)/ ν (C ¹³ O)
1810/1730	ν (CO)/ ν (C ¹³ O)
1630	δ (OH)

organic species we could find using FTIR during cyclic voltammetry (Figure 2a). It can be detected from a potential around 0.2 V and accumulates up to the start of the electrochemical reaction at 0.45 V (Figure 2b).

In addition to the potentiodynamic measurements, also potentiostatic CA curves were recorded to evaluate whether the surface coverage of CO increases with time and might be responsible for the recorded current drop. A potential of 0.77 V was chosen for in situ FTIR CA measurements because this value is in the range of the methanol electrooxidation and near the maximum value of the current. The results for both spectroscopy and electrochemistry are displayed in Figure 3. The FTIR spectra reveal three IR bands located at 1630, 1850, and 2020 cm⁻¹ which can be assigned to OH and CO similar to the results from the CV measurement. The corresponding integrated areas of both CO IR bands are displayed together with the CA curve, as shown in Figure 3b. The change in CO coverage provides information about its poisoning character. CO only accumulates at the beginning of the electrochemical reaction but not over time. The surface coverage with CO is constant as a function of time during the experiments of 100 s. The same behavior can be found for potentials lower than 0.77 V (Figure S4b in the Supporting Information). The adsorbed CO amount is constant, whereas the current decay occurs. For potentials higher than 0.77 V, the amount of CO decreases with time. However, also the associated CA curve reveals a different curve form (Figure S4a in the Supporting Information). The current density rapidly declines during the first 200 s before proceeding with a more flat slope. We assume that this could be correlated to a reduced active surface because of the formation of platinum oxides. Thus, hypothesis one, assuming blocking intermediates as the cause of the continuous current loss, cannot explain the current–time behavior of the alkaline MOR.

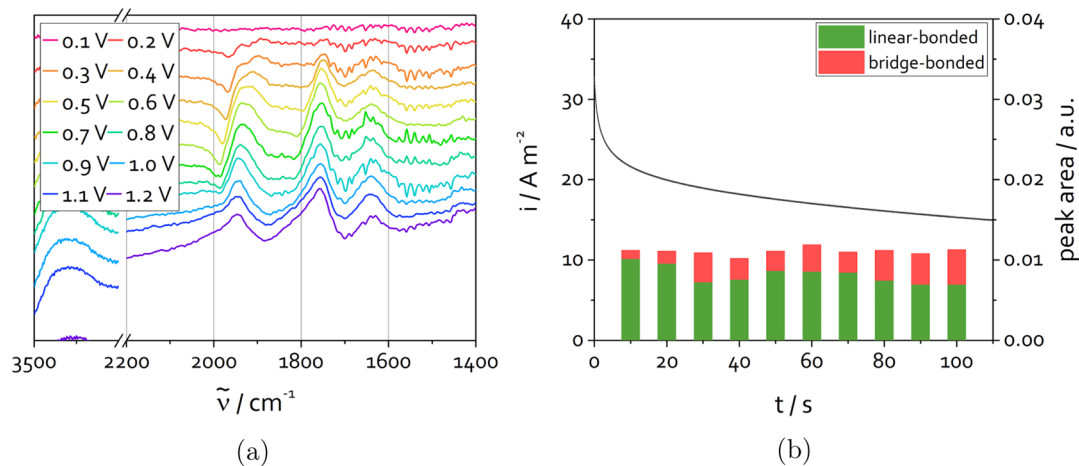


Figure 3. (a) In situ FTIR spectra of a 0.1 M NaOH + 0.1 M MeOH solution on a thin platinum film catalyst during potentiostatic measurement at 0.77 V. (b) Corresponding current–time curves and the integrated IR band intensities of adsorbed bridge and linear bonded CO at 0.77 V.

Hypothesis Two: Electrolyte Composition. The second hypothesis assumes that a change in the electrolyte composition because of the consumption of hydroxide ions causes the continuous decline in current density. The complete oxidation of methanol to CO₂ requires six hydroxide ions. When CO₂ further reacts to carbonate, two additional hydroxide ions are consumed. This high OH⁻ consumption might result in a local pH shift at the electrode.

Chronoamperometric measurements of the alkaline methanol solution with partial or complete replacement by deuterated species, which are shown in Figure 4, demonstrate

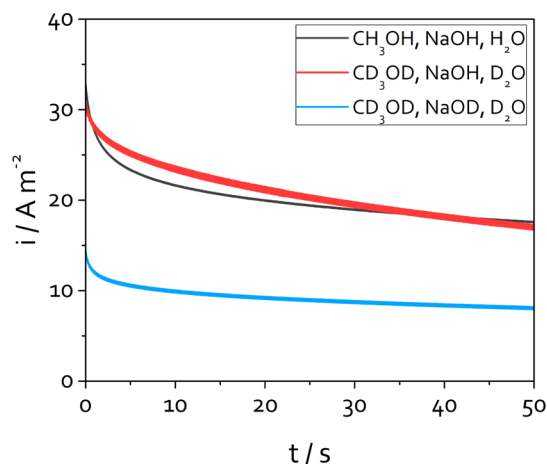


Figure 4. Current–time curve of alkaline methanol solutions using different combinations of deuterated species at 0.77 V on a thin Pt film. All sodium and methanol concentrations were set to 0.1 M. Blue: no deuterated species, red: methanol and water are deuterated, green: all three components are completely deuterated.

that the influence of the electrolyte on the current is indeed a key factor. Because deuterated species have higher molar masses compared to the non deuterated form, they lower the kinetics and influence the reaction rate. Two different systems were studied, one replacing methanol and water with their deuterated type and another where all three compounds (NaOH, MeOH, and H₂O) are in their deuterated form. The change of methanol and water to CD₃OD and D₂O has hardly any influence on the current–time response. With a suitable

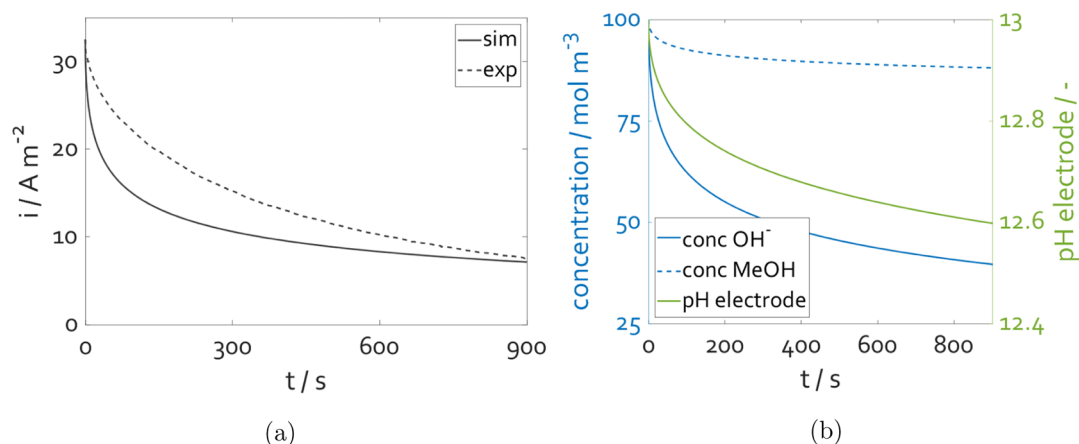


Figure 5. (a) Simulated and experimental current–time curves of a 0.1 M NaOH + 0.1 M MeOH solution at a Pt RDE with an applied potential of 0.77 V. (b) Simulated concentration (OH and MeOH) and pH with the same parameters.

source of D, a hydrogen–deuterium exchange can take place according to the reaction: $\text{OH}^- + \text{D}_2\text{O} \rightarrow \text{OD}^- + \text{HDO}$. D_2O should theoretically work as a source for such an exchange with NaOH. Because the current–time response is almost identical in the electrolytes with H_2O (Figure 4, blue line) and D_2O (Figure 4, red line), either the exchange does not take place or the amount of OH^- from NaOH is sufficient for the alkaline MOR and does not harm the kinetics. Grabowski et al. investigated rate constants of H/D exchange reactions.³² They found different factors which are responsible for the exchange but also described exceptions where a transfer of deuterium was expected but did not occur. Because the amount of water molecules compared to sodium hydroxide is much higher, the influence of an exchange of deuterium on the current–time curves would be strong. Therefore, we conclude that the hydrogen–deuterium exchange between D_2O and NaOH takes place very slowly or not at all. Adding NaOD instead of NaOH, so that all species are completely deuterated, results in significantly lower current values because of slower kinetics based on the involvement of hydroxide ions in the rate determining step.

One of the first reports of the importance of local pH consideration was published by Kuhn and Chan in 1983.³³ They stated that the local pH change mostly occurs as a consequence of depletion or accumulation of ions in the vicinity of the electrodes and is valid for all areas of electrochemistry. Other research groups such as Gupta et al. have studied local pH effects.³⁴ They found that in CO_2 electroreduction, the local pH can be up to 6 units higher than the pH value in the bulk solution. Strbac presented results of the influence of the surface pH on the running mechanistic pathways of oxygen reduction.³⁵ A four electron pathway dominates the reduction reaction at very low and high pH values, whereas in the intermediate pH range less than four electrons will be transferred. With regard to the alkaline MOR, a local pH shift influences the Nernst potential. In addition, the improvement of the reaction kinetic when using strong alkaline media might be reduced because the local surrounding gets lower pH and the main reaction pathway might change.^{3,4}

The use of an RDE allows one to establish a diffusion layer of defined thickness so that accumulation of ions can be studied. The results of the simulation and RDE experiment from a 0.1 M NaOH + 0.1 M MeOH solution at a potential of 0.77 V are presented in Figure 5. The CA curve of the

simulated and experimental current density data are shown in Figure 5a, whereas 5b contains the simulated concentration changes of OH^- and MeOH at the surface and the change of the pH value. During the first 900 s, the simulated hydroxide concentration falls by more than 60% which corresponds to a local pH shift from 13 to 12.6. Both experimental and simulated current density decrease by around 75% during the first 900 s. In the beginning, the simulated curve declines faster than the experimental one. The reason for the deviation might be that the model is based on a simplified description of the kinetics and transport. While a comprehensive model that covers all aspects of the reaction is out of scope here, the following factors may contribute to the deviation. Mass transfer conditions could deviate from the model assumptions. A not completely smooth catalyst surface or disturbances of the flow induced by the walls of the RDE measurement cell might lead to a nonideal concentration boundary layer. Moreover, migrative transport was neglected because of the high conductivity of the electrolyte. Another cause might be the reaction mechanism of the methanol oxidation. The complete oxidation of methanol to CO_2 is implemented in the model, and it is assumed that the CO_2 reacts with two additional hydroxide ions to form carbonate. Thus, eight hydroxide ions are consumed per six exchanged electrons. However, carbonation may not be in equilibrium, which would explain occurrence of bicarbonate.³⁶ Furthermore, in a previous publication we could show that under certain conditions, a share of the total current results from the incomplete oxidation of methanol to formaldehyde.³⁷ In this case, one hydroxide ion is consumed per exchanged electron. Thus, the simulation provides an upper limit for the pH effect. All the effects discussed so far would lead to an increased mass transfer or a reduced consumption of hydroxide. Thus, it is reasonable that the simulated curve lies below the experimental one.

Altogether, the simulation clarifies that even small pH changes can lead to large deviations in the current and therefore must be considered for stationary measurements of alkaline methanol oxidation. The simulations also show that the concentration changes in the electrolyte take a considerable amount of time even in an RDE setup and can explain a current decay that continues for more than 15 min. The comparison of the simulation with the experimental data shows that a pH shift is able to explain a large part of the current loss and therefore is an important effect which reduces

the current density of the alkaline methanol oxidation. This was also proven for higher concentrations (0.5 M, Figure S5 in Supporting Information) because these concentrations are closer to the conditions in an ADMFC, as well as for different potentials (Figure S6 in Supporting Information) and rotation rates (Figure S7 in Supporting Information).

CONCLUSIONS

In summary, our work presents the investigation of two hypotheses to explain the continuously current density decay of the alkaline MOR under potentiostatic conditions. Identifying the underlying causes might help to identify better conditions for stable, high performance of such electrodes. The combination of electrochemical and spectroscopic measurements reveals that hypothesis one, which describes the contribution of blocking reaction intermediates is not valid to explain the drop under the investigated conditions. Carbon monoxide was the only intermediate which could be found by FTIR spectroscopy in the potential range of the alkaline MOR. Because the amount of CO did not change with time at fixed potentials, there have to be other effects influencing the current.

Hypothesis two focuses on the influence of the electrolyte because of the consumption of hydroxide ions and methanol. Measurements with deuterated species show that the influence of OH⁻ concentration is much higher than that of methanol. The influence of a pH shift caused by the electrochemical reaction itself on the current density was analyzed with a physicochemical model. This pH shift was simulated for a system with an one electron transfer as the rate determining step. The present model results strongly support the hypothesis of a significant impact of the pH change on the current density but only at potentials where a current density is reached. The slight deviations between the experiment and simulation may result from the simplifying model assumption and might be reduced by a systematic extension of the model including nonidealities, intermediates, and slow carbonation. In the future, it would be of great interest to measure the local pH which could be done by measurements with microelectrodes to gain further insights into local concentration changes near the electrode surface.^{38–40}

ASSOCIATED CONTENT

Supporting Information

The Supporting Information is available free of charge at <https://pubs.acs.org/doi/10.1021/acsami.0c06547>.

Band shift (FTIR), potential–pH (Pourbaix) diagram, experimental cyclic voltammograms, in situ FTIR spectra, and current time curves (ZIP)

Band shift (FTIR), potential–pH (Pourbaix) diagram, experimental cyclic voltammograms, in situ FTIR spectra, and current time curves (PDF)

AUTHOR INFORMATION

Corresponding Author

Ulrike Krewer – Institute of Energy and Process Systems Engineering, TU Braunschweig, 38106 Braunschweig, Germany; Institute for Applied Materials, Karlsruhe Institute of Technology, 76131 Karlsruhe, Germany; orcid.org/0000-0002-5984-5935; Phone: +49 721 608 47491; Email: ulrike.krewer@kit.edu

Authors

Theresa Haisch – DECHEMA Research Institute, 60486 Frankfurt am Main, Germany; Institute of Energy and Process Systems Engineering, TU Braunschweig, 38106 Braunschweig, Germany; orcid.org/0000-0003-0734-479X

Fabian Kubannek – Institute of Energy and Process Systems Engineering, TU Braunschweig, 38106 Braunschweig, Germany

Dejun Chen – Department of Chemistry, Georgetown University, Washington, District of Columbia 20007, United States; orcid.org/0000-0002-8426-9941

YuYe J. Tong – Department of Chemistry, Georgetown University, Washington, District of Columbia 20007, United States; orcid.org/0000-0003-2799-022X

Notes

The authors declare no competing financial interest.

ACKNOWLEDGMENTS

This work was financially supported by the Deutsche Forschungsgemeinschaft (ADMFC/AOBJ: 622591) and by the Department of Defense, the Army Research Office (66191 CH).

REFERENCES

- (1) Bertau, M.; Offermanns, H.; Plass, L.; Schmidt, F.; Wernicke, H. *Methanol: The Basic Chemical and Energy Feedstock of the Future*; Springer: Heidelberg, 2014.
- (2) Carpenter, A. R.; Hinze, P. C. System safety analysis of hydrogen and methanol vehicle fuels. *Process Saf. Prog.* **2004**, *23*, 292–299.
- (3) Prabhuram, J.; Manoharan, R. Investigation of methanol oxidation on unsupported platinum electrodes in strong alkali and strong acid. *J. Power Sources* **1998**, *74*, 54–61.
- (4) Antolini, E.; Gonzalez, E. R. Alkaline direct alcohol fuel cells. *J. Power Sources* **2010**, *195*, 3431–3450.
- (5) Bliznac, B. B.; Ross, P. N.; Markovic, N. M. Oxygen electroreduction on Ag (111): The pH effect. *Electrochim. Acta* **2007**, *52*, 2264–2271.
- (6) Haisch, T.; Kubannek, F.; Baranton, S.; Coutanceau, C.; Krewer, U. The influence of adsorbed substances on alkaline methanol electrooxidation. *Electrochim. Acta* **2019**, *295*, 278–285.
- (7) Matsuoka, K.; Iriyama, Y.; Abe, T.; Matsuoka, M.; Ogumi, Z. Electro oxidation of methanol and ethylene glycol on platinum in alkaline solution: Poisoning effects and product analysis. *Electrochim. Acta* **2005**, *51*, 1085–1090.
- (8) Haisch, T.; Kubannek, F.; Nikitina, L.; Nikitin, I.; Pott, S.; Clees, T.; Krewer, U. The origin of the hysteresis in cyclic voltammetric response of alkaline methanol electrooxidation. *Phys. Chem. Chem. Phys.* **2020**, *22*, 16648.
- (9) Pourbaix, M. J. N.; Van Muylder, J.; de Zoubov, N. Electrochemical properties of the platinum metals. *Platin. Met. Rev.* **1959**, *3*, 47–53.
- (10) Mayrhofer, K. J. J.; Wiberg, G. K. H.; Arenz, M. Impact of Glass Corrosion on the Electrocatalysis on Pt Electrodes in Alkaline Electrolyte. *J. Electrochem. Soc.* **2008**, *155*, P1.
- (11) Mayrhofer, K. J. J.; Crampton, A. S.; Wiberg, G. K. H.; Arenz, M. Analysis of the Impact of Individual Glass Constituents on Electrocatalysis on Pt Electrodes in Alkaline Solution. *J. Electrochem. Soc.* **2008**, *155*, P78.
- (12) Iwasita, T. *Handbook of Fuel Cells—Fundamentals, Technology and Applications*; John Wiley & Sons, 2003; pp 603–624.
- (13) Lai, S. C. S.; Kleijn, S. E. F.; Öztürk, F. T. Z.; van Rees Vellinga, V. C.; Koning, J.; Rodriguez, P.; Koper, M. T. M. Effects of electrolyte pH and composition on the ethanol electro oxidation reaction. *Catal. Today* **2010**, *154*, 92–104.

- (14) Figueiredo, M. C.; Arán Ais, R. M.; Climent, V.; Kallio, T.; Feliu, J. M. Evidence of local pH changes during ethanol oxidation at Pt electrodes in alkaline media. *ChemElectroChem* **2015**, *2*, 1254–1258.
- (15) Morallón, E.; Rodes, A.; Vázquez, J. L.; Pérez, J. M. Voltammetric and in situ FTIR spectroscopic study of the oxidation of methanol on Pt (hkl) in alkaline media. *J. Electroanal. Chem.* **1995**, *391*, 149–157.
- (16) Zhou, Z. Y.; Tian, N.; Chen, Y. J.; Chen, S. P.; Sun, S. G. In situ rapid scan time resolved microscope FTIR spectroelectrochemistry: study of the dynamic processes of methanol oxidation on a nanostructured Pt electrode. *J. Electroanal. Chem.* **2004**, *573*, 111–119.
- (17) John, S. S.; Atkinson, R. W.; Roy, A.; Unocic, R. R.; Papandrew, A. B.; Zawodzinski, T. A. The effect of carbonate and pH on hydrogen oxidation and oxygen reduction on Pt Based electrocatalysts in alkaline media. *J. Electrochem. Soc.* **2016**, *163*, F291–F295.
- (18) Krewer, U.; Weinzierl, C.; Ziv, N.; Dekel, D. R. Impact of carbonation processes in anion exchange membrane fuel cells. *Electrochim. Acta* **2018**, *263*, 433–446.
- (19) Schröder, D.; Krewer, U. Model based quantification of air composition impact on secondary zinc air batteries. *Electrochim. Acta* **2014**, *117*, 541–553.
- (20) Chen, D. J.; Tong, Y. J. Irrelevance of carbon monoxide poisoning in the methanol oxidation reaction on a PtRu electrocatalyst. *Angew. Chem., Int. Ed.* **2015**, *54*, 9394–9398.
- (21) Chen, D. J.; Allison, T. C.; Tong, Y. J. Mechanistic insights into electro oxidation of solution CO on the polycrystalline gold surface as seen by in situ IR spectroscopy. *J. Phys. Chem. C* **2016**, *120*, 16132–16139.
- (22) Tripković, A. V.; Popović, K. D.; Lović, J.; Jovanović, V.; Kowal, A. Methanol oxidation at platinum electrodes in alkaline solution: comparison between supported catalysts and model systems. *J. Electroanal. Chem.* **2004**, *572*, 119–128.
- (23) Srinivasan, S. *Fuel Cells: From Fundamentals to Applications*; Springer Science & Business media, 2006.
- (24) Röhe, M.; Kubanek, F.; Krewer, U. Processes and Their Limitations in Oxygen Depolarized Cathodes: A Dynamic Model Based Analysis. *ChemSusChem* **2019**, *12*, 2373–2384.
- (25) Lee, S. H.; Rasaiah, J. C. Proton transfer and the mobilities of the H⁺ and OH⁻ ions from studies of a dissociating model for water. *J. Chem. Phys.* **2011**, *135*, 124505.
- (26) Levich, V. G. *Physicochemical Hydrodynamics*; Prentice Hall: N.J., 1962.
- (27) Noda, K.; Ohashi, M.; Ishida, K. Viscosities and densities at 298.15 K for mixtures of methanol, acetone, and water. *J. Chem. Eng. Data* **1982**, *27*, 326–328.
- (28) Tripković, A. V.; Popović, K.; Momčilović, J.; Draić, D. Kinetic and mechanistic study of methanol oxidation on a Pt (111) surface in alkaline media. *J. Electroanal. Chem.* **1996**, *418*, 9–20.
- (29) Beden, B.; Lamy, C.; Bewick, A.; Kunimatsu, K. Electrosorption of methanol on a platinum electrode. IR spectroscopic evidence for adsorbed CO species. *J. Electroanal. Chem. Interfacial Electrochem.* **1981**, *121*, 343–347.
- (30) Corrigan, D. S.; Leung, L. W. H.; Weaver, M. J. Single potential alteration surface infrared spectroscopy: examination of adsorbed species involved in irreversible electrode reactions. *Anal. Chem.* **1987**, *59*, 2252–2256.
- (31) Lane, G. S.; Miller, J. T.; Modica, F. S.; Barr, M. K. Infrared spectroscopy of adsorbed carbon monoxide on platinum/nonacidic zeolite catalysts. *J. Catal.* **1993**, *141*, 465–477.
- (32) Grabowski, J. J.; DePuy, C. H.; Bierbaum, V. M. Gas phase hydrogen deuterium exchange reactions of hydroxide and hydroxide ions with weakly acidic neutrals. *J. Am. Chem. Soc.* **1983**, *105*, 2565–2571.
- (33) Kuhn, A. T.; Chan, C. Y. pH changes at near electrode surfaces. *J. Appl. Electrochem.* **1983**, *13*, 189–207.
- (34) Gupta, N.; Gattrell, M.; MacDougall, B. Calculation for the cathode surface concentrations in the electrochemical reduction of CO₂ in KHCO₃ solutions. *J. Appl. Electrochem.* **2006**, *36*, 161–172.
- (35) Strbac, S. The effect of pH on oxygen and hydrogen peroxide reduction on polycrystalline Pt electrode. *Electrochim. Acta* **2011**, *56*, 1597–1604.
- (36) Mitchell, M. J.; Jensen, O. E.; Cliffe, K. A.; Maroto Valer, M. M. A model of carbon dioxide dissolution and mineral carbonation kinetics. *Proc. R. Soc. A* **2009**, *466*, 1265–1290.
- (37) Haisch, T.; Kubanek, F.; Haisch, C.; Bahnemann, D. W.; Krewer, U. Quantification of formaldehyde production during alkaline methanol electrooxidation. *Electrochem. Commun.* **2019**, *102*, 57.
- (38) de Hemptinne, A. Intracellular pH and surface pH in skeletal and cardiac muscle measured with a double barrelled pH microelectrode. *Pfluegers Arch.* **1980**, *386*, 121–126.
- (39) Lewandowski, Z.; Lee, W. C.; Characklis, W. G.; Little, B. Dissolved oxygen and pH microelectrode measurements at water immersed metal surfaces. *Corrosion* **1989**, *45*, 92–98.
- (40) Botz, A.; Clausmeyer, J.; Öhl, D.; Tarnev, T.; Franzen, D.; Turek, T.; Schuhmann, W. Local Activities of Hydroxide and Water Determine the Operation of Silver Based Oxygen Depolarized Cathodes. *Angew. Chem., Int. Ed.* **2018**, *57*, 12285–12289.